Integration of GPS and Tiltmeters for Structure Monitoring

Wentao YANG* Xiaoli DING* and Youlin XU**
*Department of Land Survey and Geo-informatics
**Department of Civil and Structural Engineering
The Hong Kong Polytechnic University
Hung Hom, Kowloon, Hong Kong
lswtyang@gmail.com, lsxlding@polyu.edu.hk, ceylxu@polyu.edu.hk

Abstract
GPS has been studied extensively in recent years for monitoring structural dynamics and deformation. The technology offers a number of advantages in such applications. It is however well known that GPS observations are often affected by error sources such as the GPS signal multipath effects especially on observation sites where there are smooth reflective surfaces such as structure surfaces on a building roof or the suspension cables on a cable stayed bridge. The errors often render the GPS observations inaccurate and unreliable. We investigate in this research into a structure monitoring system where GPS and a tiltmeter are integrated on a common platform so that the GPS and the tiltmeter measurements can be integrated. Since the error sources of GPS and the tiltmeters are different, the combined system makes good use of the complementary natures of the sensors to derive better monitoring results. The integrated system, the data processing and analysis involved and some experimental results are presented.

Keywords: GPS, Tiltmeter, Structure Monitoring

1. Introduction

Global Positioning System (GPS) has become a useful tool for monitoring deformation and dynamics of structures, such as dams, bridges and high-rise buildings[4],[5],[6],[11],[12],[13],[14],[15]. However, GPS positioning accuracy in such applications is highly sensitive to multipath effects that occur when GPS signals reflected by nearby objects arrive at a receiver's antenna[22]. In addition, for high-rise structure monitoring, the tropospheric effects cannot be effectively mitigated by the double-difference operations in GPS data processing[7]. Errors from the multipath and tropospheric effects can often become significant for structure monitoring applications.

GPS carrier-phase multipath effects can be avoided or reduced, for instance, by using multipath-rejecting GPS antennas (e.g. advanced pinwheel compact controlled reception pattern antenna[9] and chokering antenna) or the so-called multipath "resistant" receivers employing correlation techniques, such as the narrow correlator spacing[19], MET[18] and MMW[2] techniques. Other post-processing techniques, such as weighting GPS observations based on signal-to-noise ratio (SNR) or carrier-to-noise power-density (C/N0)[1],[3], and using various filtering approaches[16],[17],[20],[21],[22]. Nevertheless, it is very difficult to mitigate multipath errors completely using any of these approaches. It is also a very challenging task to model and mitigate the tropospheric effects when high-rise buildings are monitored[7].

We will present in this paper an integrated structure monitoring system consisting of a multi-antenna GPS system and a dual-axial tiltmeter. The system makes use of the

complementary natures of GPS and tiltmeter measurements to derive accurate structural deformation information.

2. Integrated Monitoring System

2.1 Hardware Components

We deploy a rigid steel platform (Figure 1) on which a dual-axial tiltmeter and three GPS antennas (A1, A2 and A3) are firmly attached. The distances between the antennas are 1 m and the tiltmeter is fixed at the centre of the triangular platform. Single frequency GPS receivers (e.g., Hemisphere SX2) and antennas are used. The accuracy of the tiltmeter is about ± 3".

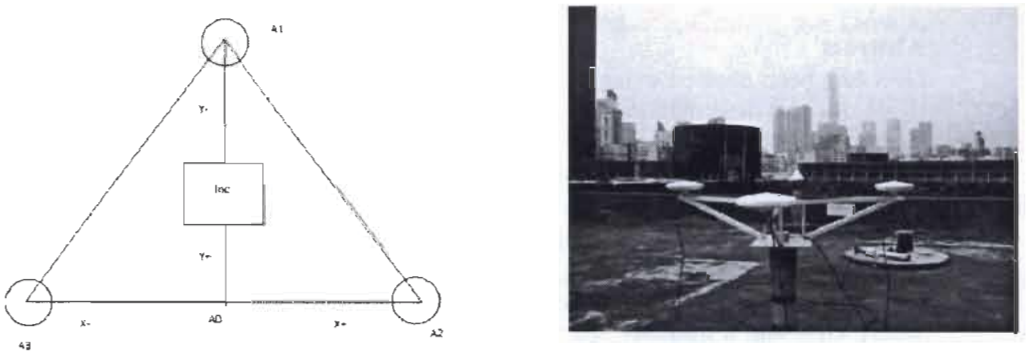

Fig. 1 Hardware components of integrated system

2.2 Observations equations

As shown in Figure 1, the tilt angles X_a and Y_a can be expressed as

$$X_a = \arcsin(\frac{H_2 - H_3}{\bar{L}_{23}})$$

$$Y_a = \arcsin(\frac{H_0 - H_1}{(\frac{\bar{L}_{12} + \bar{L}_{13}}{2}) * \sin(\pi/3)}) \quad (1)$$

where X_a and Y_a are the tilt angle measurements along the X and the Y axis of the tiltmeter, respectively; H_i $(i = 0, 1, 2, 3)$ is the elevation of point Ai, and $\bar{L}_{12}$ and $\bar{L}_{13}$ are the known distances between antennas A1 and A2 as well as between A1 and A3.

The longitude, latitude and elevation of a point can be computed from the geocentric Cartesian coordinates X_i, Y_i, Z_i,

$$\begin{bmatrix} L \\ B \\ H \end{bmatrix} = \begin{bmatrix} \arctan(\frac{Y}{X}) \\ \arctan\{\frac{Z(N+H)}{\sqrt{(X^2+Y^2)[N(1-e^2)+H)}}\} \\ \frac{Z}{\sin B} - N(1-e^2) \end{bmatrix} \quad (2)$$

$$N = \frac{a}{\sqrt{1 - e^2 \sin^2 B}}$$

where a is the semi-major axis and e is the eccentricity of the ellipsoid. Considering Equations (1) and (2), we can get

$$X_a = \arcsin\left(\frac{\frac{Z_2}{\sin B_2} - \frac{Z_3}{\sin B_3} - G}{\bar{L}_{23}}\right)$$

$$Y_a = \arcsin\left(\frac{\frac{Z_3}{2\sin B_3} + \frac{Z_2}{2\sin B_2} - \frac{Z_1}{\sin B_1} - F}{(\frac{\bar{L}_{12} + \bar{L}_{13}}{2}) * \sin(\pi/3)}\right) \quad (3)$$

where

$$G = \frac{a}{\sqrt{1 - e^2 \sin^2 B_2}}(1 - e^2) - \frac{a}{\sqrt{1 - e^2 \sin^2 B_3}}(1 - e^2)$$

$$F = \left(\frac{a}{2\sqrt{1 - e^2 \sin^2 B_3}} + \frac{a}{2\sqrt{1 - e^2 \sin^2 B_2}} - \frac{a}{\sqrt{1 - e^2 \sin^2 B_1}}\right)(1 - e^2)$$

Linearise the equation for the Y axis, we can get

$$Y_a^0 + V_Y = \frac{\partial Y_a}{\partial Z_1} dZ_1 + \frac{\partial Y_a}{\partial Z_2} dZ_2 + \frac{\partial Y_a}{\partial Z_3} dZ_3 + \bar{Y}_a$$

$$V_Y + w_Y = \frac{\frac{dZ_3}{2\sin(B_3)} + \frac{dZ_2}{2\sin(B_2)} - \frac{dZ_1}{\sin(B_1)}}{\sqrt{K}} \quad (4)$$

where

$$K = \left(\left(\frac{\bar{L}_{12} + \bar{L}_{13}}{2}\right) * \sin(\pi/3)\right)^2 - \left(\frac{Z_3}{2\sin B_3} + \frac{Z_2}{2\sin B_2} - \frac{Z_1}{\sin B_1} - F\right)^2;$$

$$w_Y = Y_a^0 - \bar{Y}_a;$$

Y_a^0 is the measured tilt angle; and $\bar{Y}_a$ is the tilt angle calculated from the initial coordinates. The observation equation for the tilt angle along the X axis can be derived similarly,

$$X_a^0 + V_X = \frac{\partial X_a}{\partial Z_3} dZ_3 + \frac{\partial X_a}{\partial Z_2} dZ_2 + \bar{X}_a$$

$$X_a^0 + V_X = \frac{1}{\bar{L}_{23}} \frac{\frac{dZ_2}{\sin(B_2)} - \frac{dZ_3}{\sin(B_3)}}{\sqrt{1 - \left(\frac{\frac{Z_2}{\sin B_2} - \frac{Z_3}{\sin B_3} - G}{\bar{L}_{23}}\right)^2}} + \bar{X}_a$$

$$V_X + w_X = \frac{\frac{dZ_2}{\sin(B_2)} - \frac{dZ_3}{\sin(B_3)}}{\sqrt{J}} \quad (5)$$

where

$$J = \bar{L}_{23}^2 - \left(\frac{Z_3}{\sin B_3} - \frac{Z_2}{\sin B_2} - G\right)^2$$

$$w_X = X_a^0 - \bar{X}_a$$

X_a^0 is the measured tilt angle; and $\bar{X}_a$ is the tilt angle calculated from the initial coordinates.

When assuming that the distances between the antennas do not change during the observations, constraints can be applied by considering the distances as highly accurate distance observations. The observation equation of the distance between point A1 and A2 can be derived,

$$L_{12} = \sqrt{(X_1 - X_2)^2 + (Y_1 - Y_2)^2 + (Z_1 - Z_2)^2}$$

$$L_{12}^0 + V_{L_{12}} = \frac{\partial L_{12}}{\partial X_1} dX_1 + \frac{\partial L_{12}}{\partial X_2} dX_2 + \frac{\partial L_{12}}{\partial Y_1} dY_1 + \frac{\partial L_{12}}{\partial Y_2} dY_2 + \frac{\partial L_{12}}{\partial Z_1} dZ_1 + \frac{\partial L_{12}}{\partial Z_2} dZ_2 + \bar{L}_{12}$$

$$V_{L_{12}} + W_{L_{12}} = \frac{X_1 - X_2}{\bar{L}_{12}} dX_1 - \frac{X_1 - X_2}{\bar{L}_{12}} dX_2 + \frac{Y_1 - Y_2}{\bar{L}_{12}} dY_1 - \frac{Y_1 - Y_2}{\bar{L}_{12}} dY_2 + \frac{Z_1 - Z_2}{\bar{L}_{12}} dZ_1 - \frac{Z_1 - Z_2}{\bar{L}_{12}} dZ_2$$

where

$$\bar{L}_{12} = \sqrt{(\bar{X}_1 - \bar{X}_2)^2 + (\bar{Y}_1 - \bar{Y}_2)^2 + (\bar{Z}_1 - \bar{Z}_2)^2}$$

$$w_{L12} = L_{12}^0 - \bar{L}_{12}$$

$\bar{L}_{12}$ is the distance calculated from the initial coordinates; and L_{12}^0 is the observed distance.

Similarly we can get,

$$V_{L_{13}} + w_{L_{13}} = \frac{X_1 - X_3}{\bar{L}_{13}} dX_1 - \frac{X_1 - X_3}{\bar{L}_{13}} dX_3 + \frac{Y_1 - Y_3}{\bar{L}_{13}} dY_1 - \frac{Y_1 - Y_3}{\bar{L}_{13}} dY_3 + \frac{Z_1 - Z_3}{\bar{L}_{13}} dZ_1 - \frac{Z_1 - Z_3}{\bar{L}_{13}} dZ_3$$

$$V_{L_{23}} + w_{L_{23}} = \frac{X_2 - X_3}{\bar{L}_{23}} dX_2 - \frac{X_2 - X_3}{\bar{L}_{23}} dX_3 + \frac{Y_2 - Y_3}{\bar{L}_{23}} dY_2 - \frac{Y_2 - Y_3}{\bar{L}_{23}} dY_3 + \frac{Z_2 - Z_3}{\bar{L}_{23}} dZ_2 - \frac{Z_2 - Z_3}{\bar{L}_{23}} dZ_3$$

where

$$\bar{L}_{13} = \sqrt{(\bar{X}_1 - \bar{X}_3)^2 + (\bar{Y}_1 - \bar{Y}_3)^2 + (\bar{Z}_1 - \bar{Z}_3)^2}$$

$$\bar{L}_{23} = \sqrt{(\bar{X}_2 - \bar{X}_3)^2 + (\bar{Y}_2 - \bar{Y}_3)^2 + (\bar{Z}_2 - \bar{Z}_3)^2}$$

$$w_{L_{13}} = L_{13}^0 - \bar{L}_{13}$$

$$w_{L_{23}} = L_{23}^0 - \bar{L}_{23}$$

3. Experiments

A full week of observations with the integrated system were carried out at the site shown in Figure 1. The data sampling rate is 1 Hz for both the GPS system and the tiltmeter. The platform was kept still during the experiments and it is also assumed that the movement of the building (a 8-storey concrete building) was insignificant. When comparing the angles measured by the tiltmeter and those calculated from GPS observations, it is seen that the tiltmeter measurements are in general much more accurate. Figure 2 shows one hour of such results.

The RMS values of the results from the GPS measurements are 0.467 and 0.674 degrees respectively in the X and Y axes while those from the tiltmeter are 0.005 and 0.004 degrees.

The variations of the distances calculated from the GPS observations are illustrated in Figure 3 where one hour data was also used. It is seen that the distances vary in general within about $\pm$10 mm.

When the elevations of the points measured from GPS system alone and from the integrated system are compared (Figures 4 and 5), it can be seen that the results can be improved in general when the integrated system is used. Figure 4 shows the results from two hours of observations while Figure 5 shows an enlarged section of the results.

Table 1 gives the statistics of the results from the whole week of observations. It is seen from the results that the accuracy of the observations were improved in all the three coordinate components while the accuracy of the elevations was improved most.

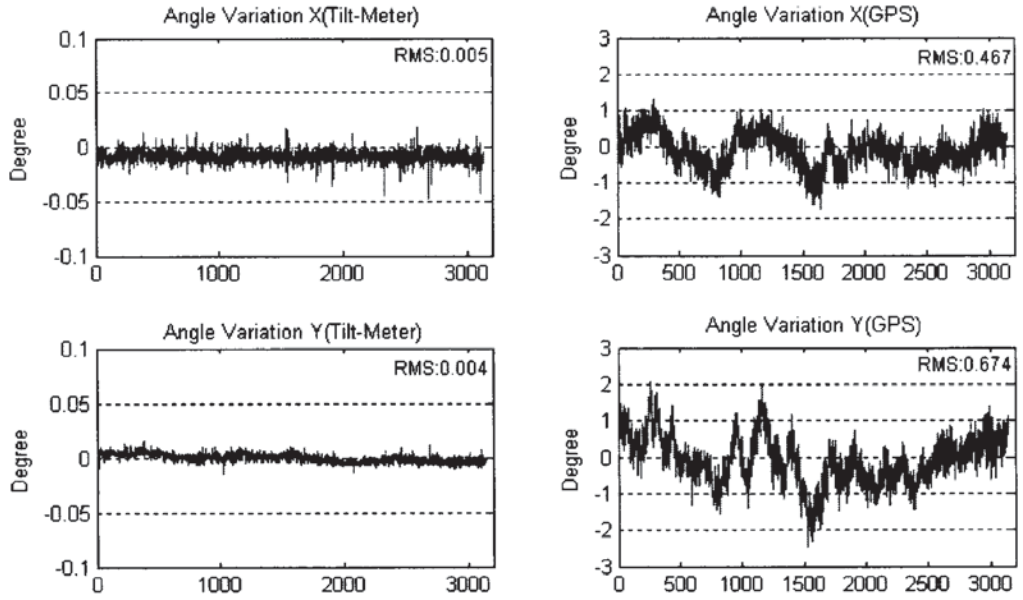

Fig. 2 Tilt angles from tiltmeter and GPS observations

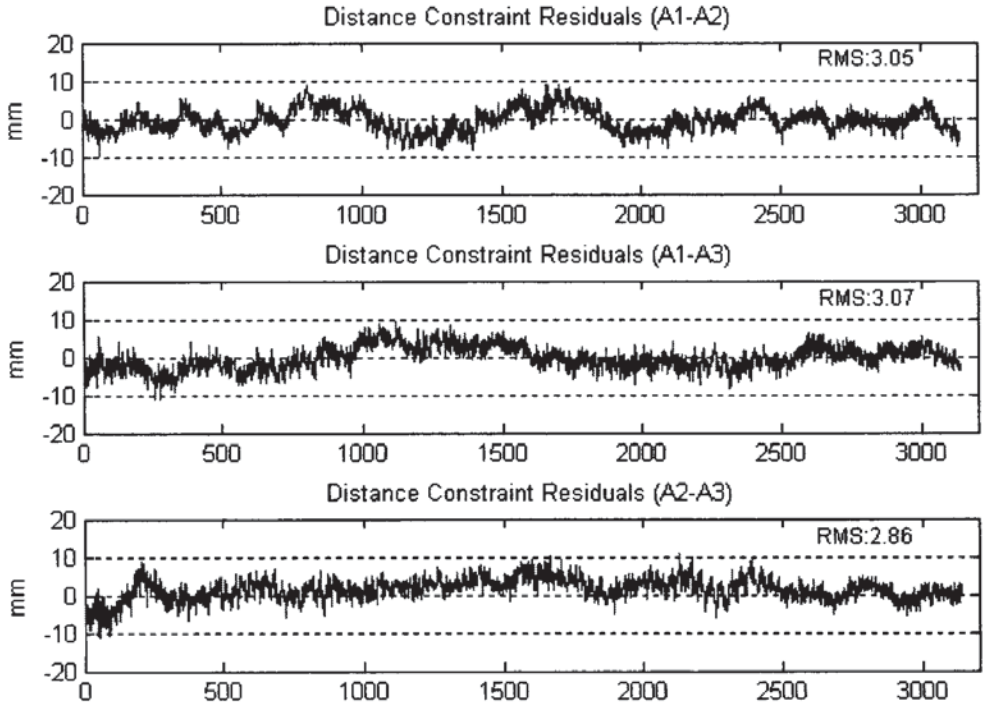

Fig. 3 Variations of distances calculated from GPS observations

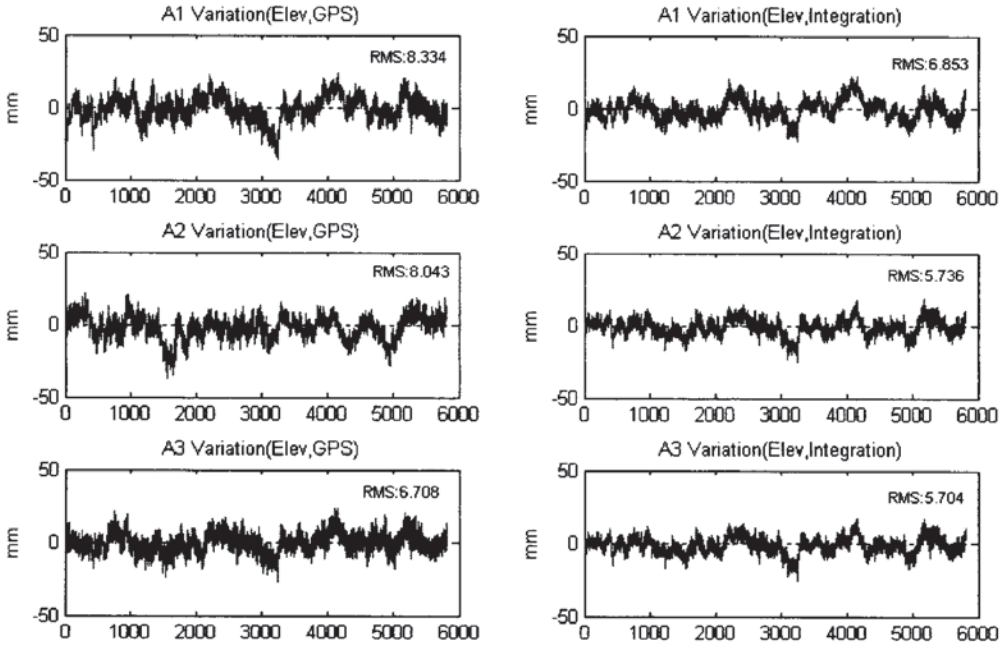

Fig. 4 Elevations from GPS observations only (left panels) and from the integrated system (right panels)

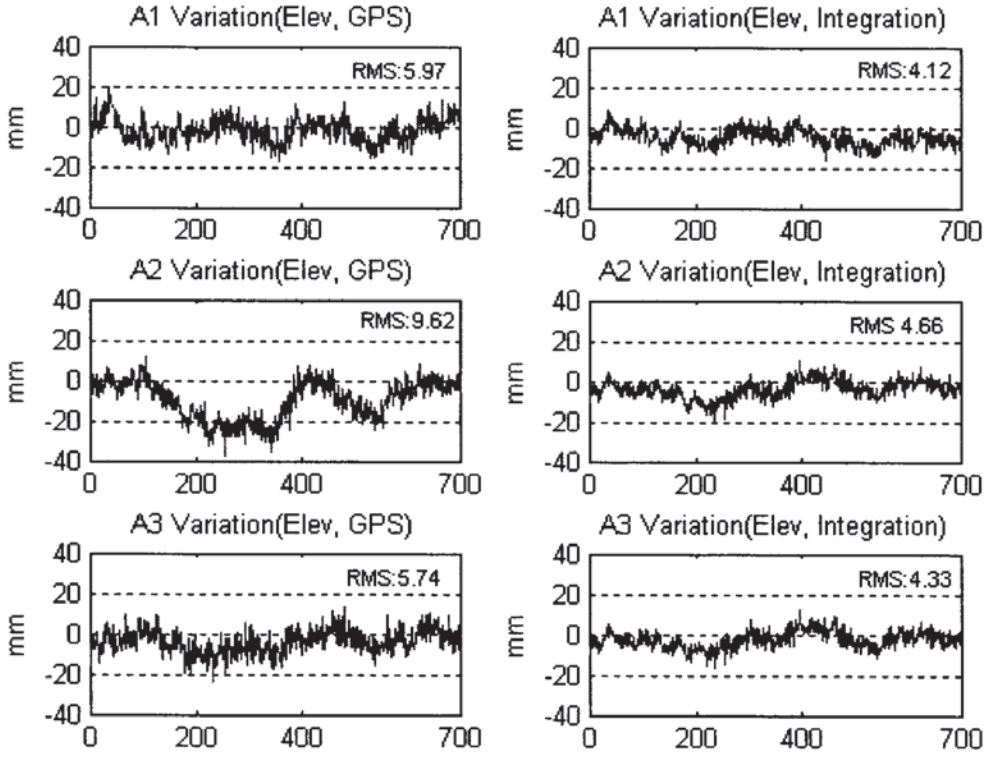

Fig. 5 Enlarged section of Fig. 4.

Table 1. RMS of coordinate variations from GPS alone and from the integrated system

		North (mm)	East (mm)	Elevation (mm)
A1	GPS	3.33	2.74	7.88
	Integration	2.72	1.90	5.14
A2	GPS	3.08	2.82	8.50
	Integration	2.22	2.24	5.38
A3	GPS	2.94	2.80	6.63
	Integration	2.22	1.88	5.23

4. Conclusions

An integrated structure monitoring system that consists of a multi-antenna GPS system and a dual-axial tiltmeter has been studied. The data processing model along with experimental results from the system have been presented. It is seen from the results that the integrated system can in general improve the observational accuracy over the GPS alone system in all the three coordinate components while the improvement in the elevation is most obvious. The integrated system should be useful in mitigating GPS observational errors such as the errors due to the GPS signal multipath and tropospheric effects.

References

(1) Axelrad, P., Comp, C.J., Macdoran, P.F. (1996) SNR-based multipath error correction for GPS differential phase. IEEE Transactions on Aerospace and Electronic Systems, 32(2):650-660.

(2) Bétaille, D.F., Cross, P.A., Euler, H.J. (2006) Assessment and improvement of the capabilities of a window correlator to model GPS multipath phase errors. IEEE Transactions on Aerospace Electronic Systems, 42(2):705-717.

(3) Brunner, F.K., Hartinger, H., Troyer, L. (1999) GPS signal diffraction modelling: the stochastic SIGMA-Δ model. Journal of Geodesy, 73:259-267.

(4) Chan WS, Xu YL, Ding XL, Dai WJ (2006) An integrated GPS-accelerometer data processing technique for structural deformation monitoring. Journal of Geodesy, 80(12):705-719.

(5) Chan, W.Y., Man, K.L. and Wong, K.Y. (2001) Real-Time Kinematic Spans the Gap, GPS World.

(6) Chen, Y.Q., Huang, D.F., Ding, X.L., Xu, Y.L., Ko, J.M. (2002) Measurement of Vibrations of Tall Buildings with GPS, Proc. of ASCE Structures Congress, 4-6 April, Denver, USA. pp. 201-202.

(7) Dai, W.J., Ding, X.L., Li, Z.W., Kwok, K.C.S., Campbell, S. (2006) Tropospheric Effects on GPS Measurements in Monitoring Tall Buildings, Location, 1(5):36-39.

(8) Kijewski-Correa, T., Kareem, A. and Kochly, M. (2006) Experimental verification and full-scale deployment of global positioning systems to monitor the dynamic response of tall buildings, Journal of Structural Engineering – ASCE, 132(8):1242-1253.

(9) Kunysz, W. (2001) Advanced pinwheel compact controlled reception pattern antenna (AP-CRPA) designed for interference and multipath mitigation. In: Proceedings of ION GPS 2001, Salt Lake City, Utah, 11-14 September, pp. 2030-2036.

(10) Li, H.N., Yi, T.H., Yi, X.D. and Wang, G.X. (2007) Measurement and analysis of wind-induced response of tall building based on GPS technology, Advances in Structural Engineering, 10(1):83-93.

(11) Lovse, J.W., Teskey, W.F., Lachapelle, G., Cannon, M.E. (1995) Dynamic deformation monitoring of tall structure using GPS technology. J Surv Eng 121(1):35-40. doi:10.1061/(ASCE)0733-9453(1995)121:1(35)

(12) Meng, X., Roberts, G.W., Dodson, A.H., Cosser, E., Barnes, J., Rizos, C. (2004) Impact of GPS satellite and pseudolite geometry on structural deformation monitoring: analytical and empirical studies. Journal of Geodesy, 77:809-822.

(13) Moschas, F. and Stiros, S. (2011) Measurement of the dynamic displacements and of the modal frequencies of a short-span pedestrian bridge using GPS and an accelerometer, Engineering Structures, 33(1):10-17.

(14) Nakamura, S. (2000) GPS measurement of wind-induced suspension bridge girder displacements. J Struct Eng 126:1413-1419.

(15) Park, H.S., Sohn, H.G., Kim, I.S. and Park, J.H. (2008) Application of GPS to monitoring of wind-induced responses of high-rise buildings, Structural Design of Tall and Special Buildings, 17(1):117-132.

(16) Satirapod, C., Rizos, C. (2005) Multipath mitigation by wavelet analysis for GPS base station applications. Survey Review, 38(295):2-10.

(17) Souza, E.M., Monico, J.F.G. (2004) Wavelet shrinkage: high frequency multipath reduction from GPS relative positioning. GPS Solutions, 8:152-159.

(18) Townsend, B., Fenton, P. (1994) A practical approach to the reduction of pseudorange multipath errors in a L1 GPS receiver. In: Proceedings of the GPS ION 94. Salt Lake City, 20-23 September, pp 143-148.

(19) van Dierendonck, A.J., Fenton, P., Ford, T. (1992) Theory and performance of narrow correlator spacing in a GPS receiver. Navigation 39(3):265-283.

(20) Zheng, D.W., Zhong, P., Ding, X.L., Chen, W. (2005) Filtering GPS timeseries using a Vondrak filter and cross-validation. Journal of Geodesy, 79:363-369.

(21) Zhong P, Ding XL, Zheng DW, Chen W, Huang DF (2008) Adaptive wavelet transform based on cross-validation method and its application to GPS multipath mitigation. GPS Solut 12:109-117. doi: 10.1007/s10291-007-0071-y

(22) Zhong, P., Ding, X.L., Yuan, L.G., Xu, Y.L., Kwok, K. and Chen, Y.Q. (2010) Sidereal filtering based on single differences for mitigating GPS multipath effects on short baselines, Journal of Geodesy, 84(2):145-158.

Acknowledgments

The research was supported by the Hong Kong Polytechnic University under a Niche Area Research Project (1-BB6B).